

Dielectric enhancement of excitons in near-surface quantum wells

L. V. Kulik and V. D. Kulakovskii

Institute of Solid State Physics, Russian Academy of Sciences, 142432 Chernogolovka, Russia

M. Bayer and A. Forchel

Technische Physik, Universität Würzburg, D-97074 Würzburg, Germany

N. A. Gippius and S. G. Tikhodeev

General Physics Institute, Russian Academy of Sciences, 117333 Moscow, Russia

(Received 15 April 1996)

The excitons in near-surface $\text{In}_x\text{Ga}_{1-x}\text{As}/\text{GaAs}$ QW's have been investigated by photoluminescence excitation and magnetophotoluminescence spectroscopy. The dielectric enhancement of excitons is demonstrated by measuring the splitting of the $2s$ and $1s$ excitons and the diamagnetic shift of the $1s$ exciton state. In agreement with theoretical calculations the exciton binding energy is found to be enhanced 1.5 times by the dielectric confinement for 5-nm-wide quantum wells with cap layer thicknesses below 3 nm. [S0163-1829(96)51828-X]

The spatial confinement of excitons in semiconductor quantum wells (QW's) enhances strongly their binding energy (E_x), as has been shown both theoretically and experimentally during the last two decades. For example, in the ideal two-dimensional (2D) limit E_x is four times larger than in bulk.¹ The enhancement of E_x has been predicted to be even stronger if the QW is surrounded by material with a smaller dielectric constant ϵ . The discontinuity of ϵ causes a redistribution of the electric fields of electron and hole. This effect is referred to as dielectric confinement and has been extensively studied in the literature,²⁻⁸ but to the best of our knowledge it has not been shown experimentally in semiconductor nanostructures.

Our paper is devoted to the experimental demonstration of dielectric confinement in QW's. The QW's were located close to vacuum with the semiconductor-vacuum (SV) interface parallel to the QW plane. On one hand, the surface introduces a strong change of the dielectric constant ϵ by one order of magnitude, which results in dielectric enhancement of the excitons in these near-surface quantum wells (NSQW's). On the other hand, in addition to the change of ϵ , the SV interface leads also to a strong change of the carrier confinement potential and therefore to an additional modification of the exciton transition energy, $\hbar\omega_{\text{ex}}$. As will be shown by calculations, this modification of $\hbar\omega_{\text{ex}}$ is even much stronger than the effect of the dielectric confinement. Consequently, studies of the excitonic transition energies in NSQW's alone, as observed in luminescence or absorption experiments, cannot give any clear manifestation of the dielectric confinement.

In the present paper we therefore investigate inner properties of excitons in NSQW's, namely, the energy gap between the $2s$ and $1s$ excitonic states, $\Delta_{12} = \hbar\omega_{\text{ex},2s} - \hbar\omega_{\text{ex},1s}$. Furthermore, we study the diamagnetic coefficient, α , which reflects the in-plane size of the $1s$ exciton. Our calculations show that any significant dependence of Δ_{12} and α on the QW cap layer thickness L_{cap} is expected only due to the dielectric confinement. Our experimental in-

vestigations of excitons in $\text{In}_x\text{Ga}_{1-x}\text{As}/\text{GaAs}$ single QW heterostructures show a rather strong increase of Δ_{12} and also a strong decrease of the diamagnetic coefficient, when the QW approaches the SV interface. These changes are therefore direct manifestations of the dielectric enhancement of excitons in the NSQW's.

For the measurements we have chosen $\text{In}_x\text{Ga}_{1-x}\text{As}/\text{GaAs}$ heterostructures with $x \sim 0.18$ and a QW thickness $L_{\text{QW}} = 5$ nm. For these QW parameters there is only one confined electron subband in the conduction band. In addition, due to the pseudomorphic growth the $\text{In}_x\text{Ga}_{1-x}\text{As}$ layer is strained, which results in a strain-induced splitting of the valence band by more than 40 meV. Therefore any spectral feature in an energy range of about 20 meV above the ground-state ($1s$) transition energy of the heavy-hole exciton is related to higher states of this exciton ($2s$, etc.). Additional advantages of the QW structures are (i) the large $\epsilon = 12$ (and therefore a decrease of ϵ at the SV interface by one order of magnitude), and (ii) the large exciton radius a_{ex} of about ~ 60 Å (and consequently a large impact of the surrounding on the exciton). The homogeneity of the QW structures was confirmed by PL spectroscopy. An as grown sample with $L_{\text{cap}} = 20$ nm was used as reference. In order to obtain samples of varying cap layer thicknesses the cap layer was thinned by etching, which avoids both surface defects and cap layer thickness fluctuations. We found that these requirements are fulfilled by dry etching with an Ar-ion beam of low ion energies (500 eV), at low sample temperature (liquid nitrogen), and with a small angle between the beam and the sample surface (20°).

The samples were immersed in liquid helium: all spectra were recorded at 4.2 K. For photoluminescence excitation (PLE) studies we have used a Ti-sapphire laser and a double-grating monochromator. A cryostat with a superconducting solenoid has been used for the photoluminescence (PL) studies. For the measurements of the exciton diamagnetic shift we have also used NSQW's that were MBE grown with $L_{\text{cap}} = 0, 1, 3, \text{ and } 16$ nm.

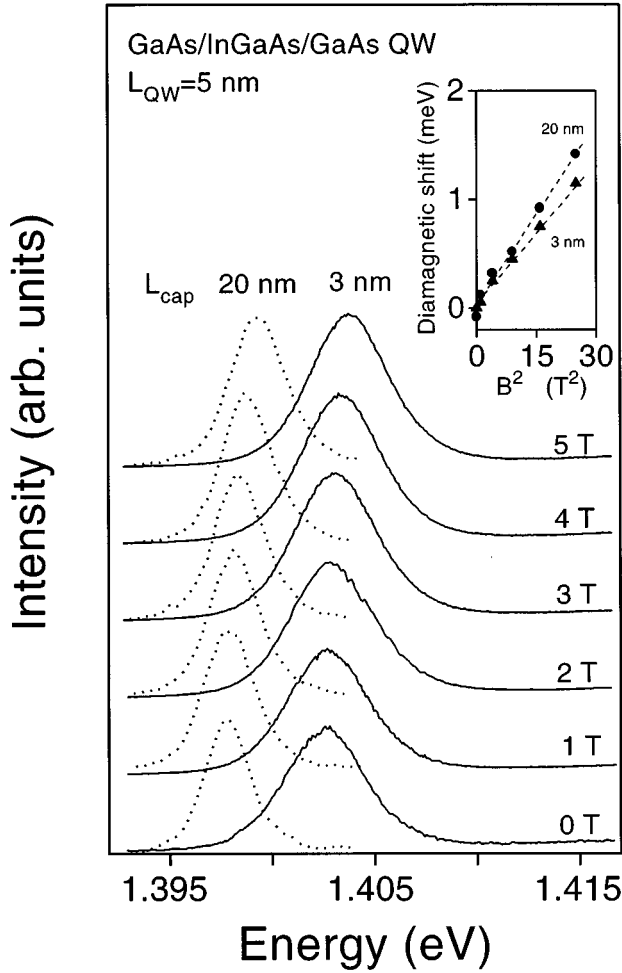


FIG. 1. Emission spectra for NSQW's with $L_{\text{cap}} = 20$ nm (dotted lines) and 3 nm (solid lines) for varying magnetic fields. The inset shows the diamagnetic shift of the exciton emission line for the same NSQW's at $B < 5$ T.

Typical PL spectra are shown in Fig. 1 for the NSQW's with $L_{\text{cap}} = 20$ nm (dotted line) and 3 nm (solid line) for magnetic fields $B \leq 5$ T. The figure shows that the etching down to 3 nm cap layer thickness results in a relatively small broadening of the exciton line indicating a high surface quality. As can be seen from the spectra at zero field (lowest traces) the decrease of the cap layer thickness leads to a pronounced shift of the exciton emission line to higher energies.

PLE spectra for the NSQW's with $L_{\text{cap}} = 20, 5,$ and 3 nm are displayed in Fig. 2 together with PL spectra. The PLE spectra show two peaks associated with 1s and 2s exciton transitions. The Stokes shift^{9,10} of the 1s exciton line between the PL and PLE spectra for varying cap layer thicknesses are very similar (about 1.5 meV). This indicates a rather weak increase of localization effects down to a cap layer thickness $L_{\text{cap}} = 3$ nm and confirms—together with the only small increase of the half-width of the emission line in PL—that the observed features are solely due to the decrease of the cap layer thickness. With decreasing cap layer thickness both the 1s and 2s exciton peaks move to higher energies. The comparison of the spectra shows that the shift of the 2s line is markedly larger than the shift of the 1s

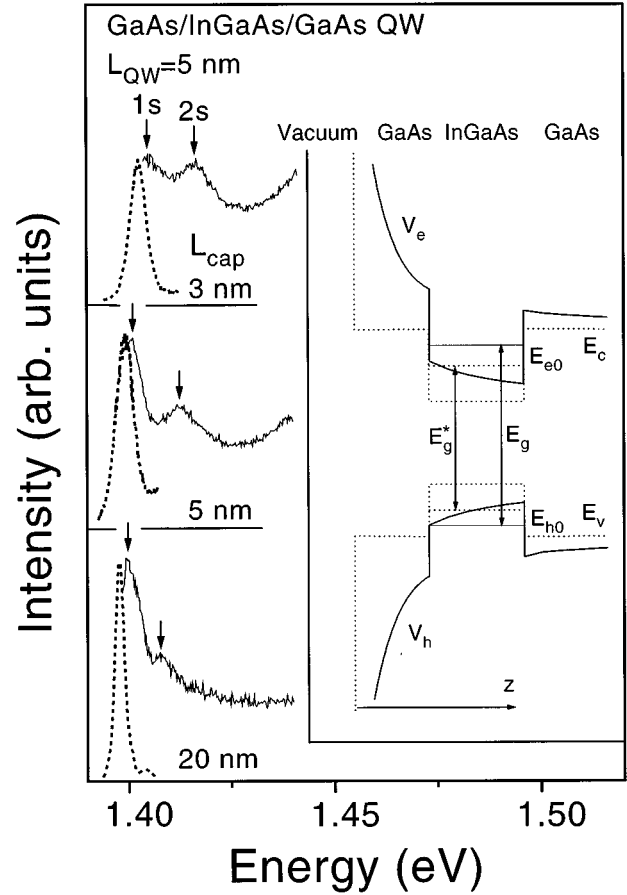


FIG. 2. PLE (solid lines) and PL (dotted lines) spectra for NSQW's with $L_{\text{cap}} = 3, 5,$ and 20 nm. The inset shows an energy scheme for the band-to-band QW transition in the NSQW's with (solid lines) and without (dotted lines) self-image charges.

exciton.¹¹ This indicates an increase of the exciton binding energy when the QW approaches the surface. Such an increase is in qualitative agreement with theoretical expectations of the dielectric enhancement of excitons.

We have also calculated the exciton energies in NSQW's as functions of L_{cap} . The SV boundary introduces a change in the barrier potential and also a discontinuity of the dielectric constant, which can be modeled by image charges. Both changes are taken into account in our calculations. To simplify the calculations we have assumed strong vertical QW confinement of the carriers. This is possible, because the QW subband splitting is significantly larger than the exciton binding energy. In this approximation, the wave function of the optically active exciton with center-of-mass momentum $K = 0$ is given by

$$\Psi_{\text{ex}}(x_e, x_h, y_e, y_h, z_e, z_h) = \psi_{\text{ex}}(x_e - x_h, y_e - y_h) \times U_e(z_e) U_h(z_h), \quad (1)$$

where ψ_{ex} describes the in-plane relative motion of the exciton. The free electron and hole ground-state wave functions $U_e(z)$ are the solutions of

$$\left[-\frac{\hbar^2}{2m_{i,\perp}} \frac{\partial^2}{\partial z_i^2} + V(z_i) \right] U_i(z_i) = E_i U_i(z_i), \quad i = e, h. \quad (2)$$

The electron and hole confining potentials V_e and V_h are given by $V_e = E_c(z_e) + V_{\text{self}}(z_e)$ and $V_h = E_v(z_h) + V_{\text{self}}(z_h)$. Here E_c and E_v are the confinement potentials in the conduction and valence bands, respectively, and

$$V_{\text{self}}(z) = \frac{e^2}{2\varepsilon} \left(\frac{\varepsilon - 1}{\varepsilon + 1} \right) \frac{1}{|2z|} \quad (3)$$

is the repulsive interaction of the carriers with their self-image charges. ε is the dielectric constant of the semiconductor for which we neglect the small difference between GaAs and $\text{In}_x\text{Ga}_{1-x}\text{As}$. z is measured from the SV boundary. The potential V_{self} results in a modification of the electron and hole confining potentials in the near surface region as shown schematically in Fig. 2. The confining potentials without ($E_{c,v}$) and with ($E_{c,v} + V_{\text{self}}$) image charges are shown by the solid and dotted lines, respectively. V_{self} induces a significant blueshift of the interband QW transition, $\Delta E = E_g - E_g^*$ which increases with decreasing cap layer thickness.

To calculate the exciton binding energies we have solved the quasi-2D exciton Schrödinger equation:

$$\left[-\frac{\hbar^2}{2\mu} \left(\frac{\partial^2}{\partial x^2} + \frac{\partial^2}{\partial y^2} \right) + \bar{V}_{eh}(x,y) \right] \psi_{\text{ex}}(x,y) = E_x \psi_{\text{ex}}(x,y) \quad (4)$$

with $\mu^{-1} = (m_e^{-1} + m_h^{-1})$ and $(x,y) = (x_e - x_h, y_e - y_h)$.

$$\bar{V}_{eh}(x,y) = \int dz_e dz_h |U_e(z_e)|^2 |U_h(z_h)|^2 V_{eh}(x,y,z_e,z_h) \quad (5)$$

is the averaged electron-hole interaction. The Coulomb interaction contains terms describing the electron-image hole interaction as well as the hole-image electron interaction

$$V_{eh}(x,y,z_e,z_h) = -\frac{e^2}{\varepsilon} \left[\frac{1}{\sqrt{x^2 + y^2 + (z_e - z_h)^2}} + \frac{\varepsilon - 1}{\varepsilon + 1} \frac{1}{\sqrt{x^2 + y^2 + (z_e + z_h)^2}} \right]. \quad (6)$$

Figures 3(a–d) display the cap layer thickness dependences of the most important exciton parameters that can be optically determined. These parameters were calculated with (solid lines) and without (dashed lines) self-image charges.¹² Figure 3(a) displays the transition energies of the $1s$ exciton $\hbar\omega_{\text{ex}}$ and of the band-to-band transitions E_g , respectively. Both increase with decreasing L_{cap} due to the increasing asymmetry of the confinement potentials $E_{c,v}$ (dashed lines) and due to the self-image charges (difference between solid and dashed lines). Moreover, Fig. 3(a) shows that the main contribution to the shift of $\hbar\omega_{\text{ex}}$ originates from the change of the confinement potential rather than from the dielectric confinement, which causes only a small additional shift to the higher energies. The influence of dielectric confinement on the exciton energy is much smaller than the influence on the free carrier energy. This difference arises from the electrical neutrality of the excitons.

The experimental values of $\hbar\omega_{\text{ex}}$ for several L_{cap} are shown in Fig. 3(a) by dots. The observed increase of $\hbar\omega_{\text{ex}}$ at

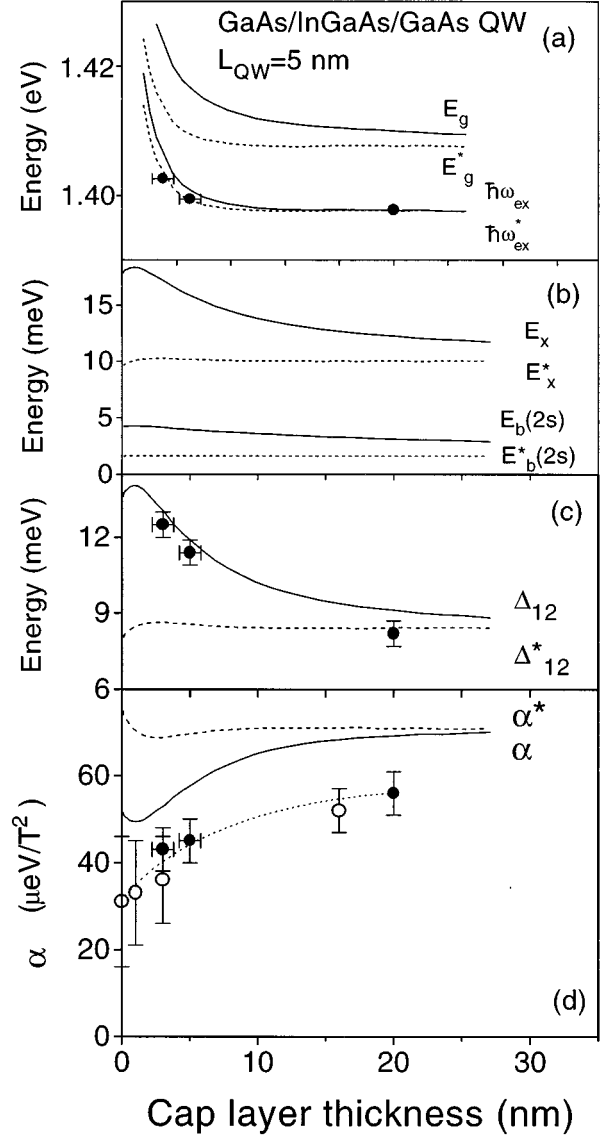


FIG. 3. Dependences of the band-to-band (E_g) and exciton ($\hbar\omega_{\text{ex}}$) transition energies (a), of the $1s$ and $2s$ exciton binding energies (b), of the energy gap between the $1s$ and $2s$ exciton states (c), and of the exciton diamagnetic coefficient (d) on the cap layer thickness in NSQW's. The dependences calculated with and without self-image charges are shown by solid and dashed lines, respectively; the latter are marked by a star. The experimental data for the QW with subsequently etched cap layer are shown by solid dots, the open dots correspond to as-grown samples. The dotted line in Fig. 3(d) connects the experimental points and is just a guide to the eye.

small L_{cap} is in qualitative agreement with the calculations. However, the rather large inaccuracy mainly in L_{cap} does not allow us to decide about the influence of dielectric confinement. This can be done by an analysis of the difference in energy between $1s$ and $2s$ exciton lines, Δ_{12} . The dashed curves in Fig. 3(b) show that the contribution to the exciton binding energy of the $1s$ and $2s$ states, which originates from the asymmetry of the potential barrier at the SV interface, is practically canceled. Therefore the dependences of E_x , $E_{x,2s}$, and Δ_{12} on L_{cap} originate only from the dielectric confinement. The solid lines in Figs. 3(b) and 3(c) show that

they increase significantly (1.5–1.8 times) when the QW approaches the SV interface. The dependence of Δ_{12} on L_{cap} appears due to the stronger influence of the image charges on the $2s$ exciton than on the $1s$ exciton, which arises from the larger size and therefore from the larger induced dipole moment of the $2s$ state.

The experimental values of Δ_{12} for varying L_{cap} are displayed in Fig. 3(c) by dots. They show a pronounced increase of Δ_{12} with decreasing L_{cap} and unambiguously demonstrate the importance of dielectric confinement in NSQW's. The calculated dependence agrees with the experimental data. The increase of Δ_{12} reaches 4 meV at $L_{\text{cap}} = 3$ nm. This corresponds to an increase of the excitonic binding energy by a factor of about 1.5. Note that Fig. 3(a) shows that the relative increase of the $2s$ state binding energy is even larger; it exceeds a factor of 2.

Another manifestation of the dielectric can be obtained from the measurement of the exciton diamagnetic shift in a magnetic field normal to the QW plane. At small magnetic fields this shift is given by $\Delta E = \alpha B^2$, in which the diamagnetic coefficient is given by $\alpha = e^2 / (8\mu) \cdot \langle r^2 \rangle$, where $\langle r^2 \rangle$ is the averaged exciton radius in the QW plane. As was shown above, the exciton binding energy and, hence, the exciton Bohr radius a_{ex} are almost independent of L_{cap} until the image charges are taken into account, but the latter lead to a significant increase of exciton binding energy and hence to a decrease of a_{ex} . Therefore the decrease of the diamagnetic shift of the exciton line in the NSQW's can also be consid-

ered as a manifestation of the dielectric enhancement.

Results of the experimental measurements are presented in the inset of Fig. 1 where typical dependences of $\Delta \hbar \omega_{\text{ex}}$ on B are shown. The results of these measurements are summarized in Fig. 3(d). The comparison of the experimental values of α (points) with the calculated ones (solid lines) in the whole range of $L_{\text{cap}} < 20$ nm is represented in Fig. 3(d). α decreases markedly by more than 30% when the QW approaches the SV interface. The relative change of α exceeds strongly its change expected from the calculations without image charges (dashed curve) and follows closely the dependence calculated with image charges (solid line).

In conclusion, we have demonstrated experimentally the strong dielectric enhancement of excitons in NSQW's by measuring both the increase of the splitting between the $2s$ and the $1s$ exciton state and the decrease of diamagnetic coefficient of the $1s$ state as the cap layer thickness decreases. Calculations of the exciton binding energies and the diamagnetic coefficient for the whole range of investigated cap layer thicknesses are in good quantitative agreement with the experiment.

We would like to thank T. Borzenko and Yu. Koval' for their assistance in etching the cap layer. The work was supported in part by INTAS (Grant No. 94-2112), by the Russian Foundation for Basic Research (Grant No. 95-02-06062a), by the Volkswagen Foundation and by the State of Bavaria.

-
- ¹G. Bastard, *Wave Mechanics Applied to Semiconductor Heterostructures* (Les Editions de Physics, Les Ulis, France, 1988), p. 138.
- ²N. S. Rytova, *Dokl. Akad. Nauk SSSR* **163**, 118 (1965) [*Sov. Phys. Dokl.* **10**, 754 (1966)].
- ³L. V. Keldysh, *Pis'ma Zh. Éksp. Teor. Fiz.* **29**, 716 (1979) [*JETP Lett.* **29**, 658 (1979)].
- ⁴E. Hanamura, N. Nagaosa, M. Kumagai, and T. Takagahara, *Mater. Sci. Eng. B* **1**, 255 (1988).
- ⁵T. Takagahara, *Phys. Rev. B* **47**, 4569 (1993).
- ⁶D. B. Tran Thoai, R. Zimmermann, M. Grundmann, and D. Bimberg, *Phys. Rev. B* **42**, 5906 (1990).
- ⁷J. Chen and K. K. Bajaj, in *Physics of Semiconductors: Proceedings of the 22nd International Conference*, edited by D. J. Lockwood, World Scientific, Vol. 2, 1324 (1994).
- ⁸E. A. Mularov, N. A. Gippius, S. G. Tikhodeev, and T. Ishihara,

Phys. Rev. B **51**, 14 370 (1995).

- ⁹J. C. Maan, G. Belle, A. Fasolino, M. Altarelli, and K. Ploog, *Phys. Rev. B* **30**, 2253 (1984).
- ¹⁰R. Dingle, in *Festkörperprobleme XV*, edited by H. J. Queisser (Vieweg, Braunschweig, 1975).
- ¹¹It should be also noted that the oscillator strength of the $2s$ exciton is strongly enhanced in comparison to that of the $1s$ exciton. The origin of this behavior is not fully understood up to now, but arises partly from the stronger enhancement of the $2s$ exciton binding energy by the dielectric confinement.
- ¹²The following parameters have been used in our calculations: GaAs: $\varepsilon = 12.5$, $m_e = 0.067m_0$, $m_{h,\perp} = 0.35m_0$. In_{0.18}Ga_{0.82}As: $\varepsilon = 12.5$, $m_e = 0.062m_0$, $m_{hh,\perp} = 0.35m_0$, $m_{hh,\parallel} = 0.2m_0$. The band offsets were chosen to be $\Delta E_c = 113$ meV in the conduction band and $\Delta E_v = 75$ meV in the valence band.